Electronic phenomena in nanodispersed thin films

1999 J. Phys.: Condens. Matter 11 9955

(http://iopscience.iop.org/0953-8984/11/49/313)

J. Phys.: Condens. Matter **11** (1999) 9955–9967. Printed in the UK PII: S0953-8984(99)04451-3

Electronic phenomena in nanodispersed thin films

R D Fedorovich, A G Naumovets† and P M Tomchuk

Institute of Physics, National Academy of Sciences of Ukraine, 46 Prospect Nauki, UA-252650, Kiev 22, Ukraine

E-mail: naumov@iop.kiev.ua

Received 21 May 1999

Abstract. We review experimental data on the electron and photon emission from island metal films (IMFs) energized by passing current or by infrared laser irradiation. A model of nonequilibrium heating of the electron gas in nanoparticles is substantiated and used to interpret the experimental results. The applications of the island metal films are also exemplified.

1. Introduction

The objects discussed in the present paper are discontinuous (island) films that are formed in the intermediate stages of growth effected by the Volmer–Weber mechanism. We will concentrate on the situation when both the size of most of the islands and the gaps between them are of the order of nanometres. Then, due to considerable electron tunnelling transparency of the nanometre potential barriers, the islands are integrated into a whole, which is reflected in the fact that the island film has a considerable conductivity. At the same time, the tunnelling probability is in any case essentially lower than unity, so the specific characteristics of individual nanoislands caused by their small size manifest themselves in collective properties of the film.

In what follows we will consider the phenomena of electron and light emission from island metal films (IMFs) energized by conduction current or by laser irradiation. The first publication about these effects occurring under the conduction current excitation appeared in 1965 [1]. The early stage of studies in this area was summarized by Borziak and Kulyupin in their monograph [2]. In recent years, IMFs have gained renewed interest in the context of the development of vacuum microelectronics and nanomaterials science. A considerable effort has been undertaken in theoretical treatment of electron kinetics in small metal particles, in a better control of the IMF structure, testing of new materials and investigation of electron emission from films exposed to infrared laser radiation. Here we will give a brief review of these works.

2. Experimental methods. Major observations and models

2.1. Preparation of island films

Island films can readily be obtained by deposition of various metals (e.g., Au, Ag, Pt, Pd, Mo, Cr, Sn, Cu) on dielectric substrates (mica, quartz, sapphire, SiO_x etc). They can also

† Corresponding author.

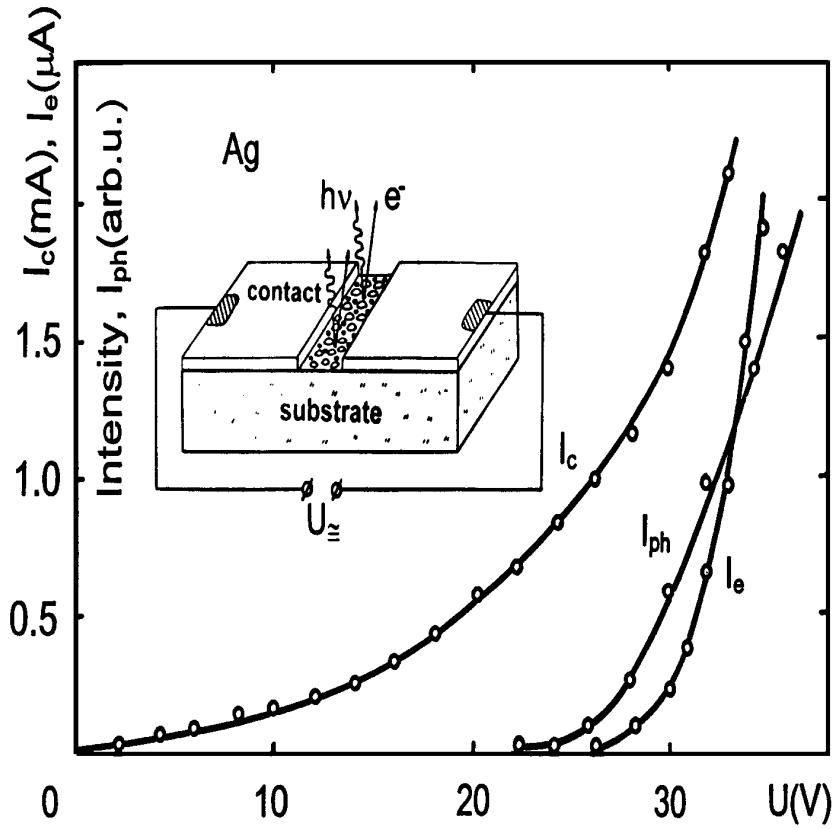

Figure 1. Conduction current (I_c), electron emission current (I_e) and intensity of the emitted light (I_{ph}) as functions of the voltage applied to a silver island film. The electron emission current is extracted to an anode placed over the film. Inset: schematic of the sample with an island film between two contact electrodes.

be prepared from graphite, metal-like compounds and semiconductors. The main criteria in deciding on a particular combination of materials are that the adsorbate should not wet the substrate and the structure of the film should remain stable under operating temperature (usually room temperature). The deposition can be performed by vacuum evaporation, cathode sputtering in a noble gas atmosphere, electrodeposition from solutions or just by spraying a suspension which contains fine solid particles [3]. Two contact electrodes, e.g. continuous Au films $\sim 10^2$ nm thick with a gap of about 10 μm between them, are prepared on the substrate prior to deposition of the island film (figure 1). The average size of the islands and their distribution over the substrate can be varied within broad limits by choosing the deposition conditions, mass thickness of the film (typically lying in the range 4–10 nm) and chemical nature of the adsorbate and substrate as well as temperature and duration of subsequent annealing.

Although this review is centred on metal island films, it is appropriate to note that there are also well developed methods of preparation of semiconductor island films (see e.g. [4, 5]).

2.2. Electroforming of IMFs

The as-deposited island films are subjected to a procedure termed *electroforming*, in which a voltage of $\sim$20–30 V is applied across the film for $\sim 10^2$ s. The current flow through the film seems to induce a process of electromigration which results in formation of well conducting percolation paths ('current channels'). High-resolution electron microscopy has shown that a current channel consists mainly of an ultradispersed system of nanoislands separated by nm distances [6]. They are linked with each other by electron tunnelling and in this way provide a continuous path in the film where a major part of the conduction current is concentrated. The current density in the channels can amount to $\sim 10^6$ A cm^{-2} [7]. The channels contain also a small number of larger islands which are shaped in the process of electroforming. The conduction current–voltage characteristics of electroformed films are non-ohmic (figure 1). The superlinear deviation from the ohmicity starts at voltages as low as $\sim$10–15 V and can reasonably be explained in terms of the tunnelling conduction mechanism [8]. The emission of electrons and photons from the IMFs starts at approximately the same voltages (figure 1). It stems from small spots which are $\leqslant 1$ μm in size and are located within the current channels. These spots are usually referred to as the *emission centres*.

2.3. Emission centres

Under an optical microscope, the light emission centres are seen as spots scattered rather chaotically over the film. The position of the electron emission centres can be visualized on a cathodoluminescent screen. The comparison of these two images shows unambiguously that electrons and photons are emitted from the same centres [9]. Electron microscopic investigations have revealed that the emission centres are located within the current channels [10]. A typical emission centre consists of a relatively large ($\approx$100 nm) island surrounded by nanosized islands [11]. It is well known that, in the course of the Ostwald ripening of dispersed systems, large particles are growing at the cost of smaller ones. Thus, the emergence of local configurations of 'a large island + nanoislands around it' should be quite probable. However, usually each channel contains no more than one centre [10]. The centres are believed to arise as a result of an intricate interplay between structure of the film and processes of electro- and thermal migration. If an enhancement of the current density appears in some place of the current channel, the electromigration, perhaps combined with somewhat enhanced resistive heating, can cause a progressive destruction of this segment of the channel. In turn, this will increase the voltage drop across this segment at the expense of the voltage drop across the remaining parts of the channel. Such an avalanche-like process appears as a kind of instability which, however, does not lead to a complete break of the channel if the voltage applied to the film is not too high. The result is that only one emission centre emerges in a channel. At some stage of the process, the film structure is stabilized through a mechanism of self-limitation, which is reflected in the fact that electroformed IMFs show stable conductivity and emission properties for thousands of hours under appropriate exploitation conditions (see section 5). An enhanced potential drop across the emission centres revealed experimentally [12] is attributed to existence of a depletion zone around a large island. This plays an important role in the electron and photon emission from IMFs, because a considerable part of the power fed into the current channel is released within the centre.

Since the island structure of the film mirrors the distribution of the nucleation centres (various defects), the shape of the current channels and their position are actually unpredictable on flat substrates which are prepared by standard methods (mechanical polishing or cleavage). Correspondingly, the emission centres are also scattered rather randomly over the film.

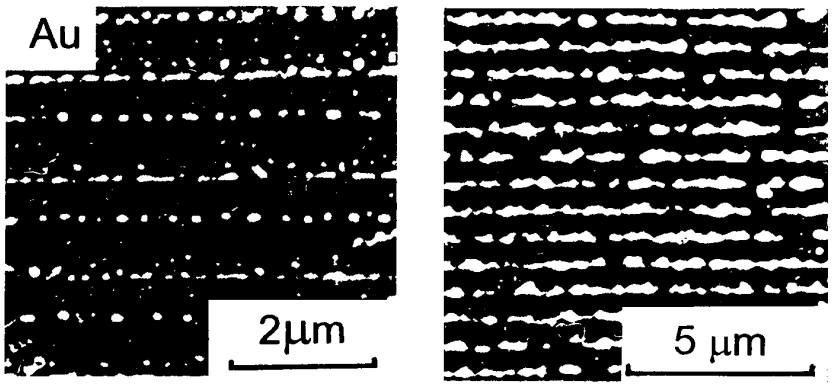

Figure 2. Electron microscopic images of chain island films on a grooved glass substrate (left) and on a corrugated surface prepared by photolithography (right).

To generate them more controllably, the film can be evaporated at a grazing angle onto a substrate whose surface is grooved (the incidence plane of the atomic beam is oriented normal to the grooves) [13, 14]. Under such an evaporation geometry, the film consists of chains of islands located in the grooves (figure 2). An island chain appears as a 'prefabricated' current channel, and actually the electroforming of the chain island films is unnecessary: electrons and light are emitted at soon as a 'normal' (not increased) operating voltage is applied to the film. However, the voltage drop along the chains appears all the same nonuniform, and the emission centre is located in the region of an enhanced voltage drop. Thus the emergence of the emission centres in the chain films seems to occur faster and at voltages below or equal to the operating voltage.

To better control the structure of the island films, one can also exploit the effect of their self-organization which occurs under proper growth conditions [4, 15]. It is understood that advances in nanotechnologies also hold much promise for tailoring the island structures (see e.g. [16]).

2.4. Models of electron emission from IMFs

Two models were suggested to explain the electron emission from the island films. The first of them, the field emission model [17], assumes that the electric field at one of the adjacent islands is high enough to cause the field emission. It is also implied that a part of the field emission current is branched off to the anode (extracting electrode) placed over the film. The phenomenon of field emission is well investigated so we will not dwell on this model at length. In fact a one-stage process is assumed in which field-emitted electrons reach the anode immediately (or maybe after a reflection from the adjacent island) (figure 3(a)). The second model, referred to as the model of hot electrons [18, 19], considers a three-stage process which involves (A) tunnelling of electrons to the adjacent island, (B) transfer of their excess energy to the electrons of the island (heating of the electron gas) and (C) emission of the hot electrons into vacuum (figure 3(b)). This model is not so obvious, especially in stage B, which assumes an efficient generation of hot electrons in small metal particles. In recent years a serious effort has been made to substantiate such a possibility [19–24]. This issue will be reviewed in the next section. Then, in section 4, we will present more experimental data on electron and light emission from IMFs and compare them with the proposed models.

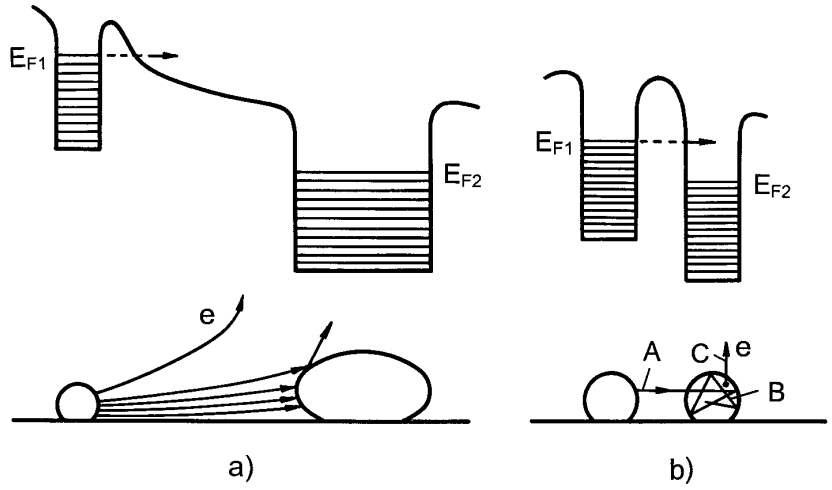

Figure 3. Illustrations of the field emission model (a) and of the model of hot electrons (b) suggested to explain the electron emission from IMFs. The potential diagrams are shown at the top and electron trajectories at the bottom (see text for explanations).

3. Hot electrons in nanoparticles (theory)

The cornerstone of the theory elaborated by one of us (PT) and aimed at the explanation of the electron and photon emission from IMFs is the substantiation of the possibility of strong nonequilibrium heating of the electron gas in small metal particles [19, 25, 26]. Until recently, hot electrons were shown to exist under stationary conditions only in gaseous and semiconductor plasmas whereas in bulk metals they can be obtained only for very short periods of time ($t < 10^{-10}$ s) [27]. The question arises of how the hot electrons can be generated in IMFs in a steady state, i.e. as long as power is fed into an IMF. To answer this question, consider a balance equation

$$Q = \alpha(T_e - T) \tag{1}$$

which links the power absorbed by the electron subsystem of a metal island, Q, with the electron and lattice temperatures, T_e and T. The coefficient α determines the intensity of electron–lattice energy transfer (strictly speaking, the equation should include higher terms in $(T_e - T)$ when this difference is large enough).

The heating process described by equation (1) can be qualitatively illustrated by a graphic model (figure 4). Suppose there are two vessels, different in cross-section, the narrow vessel being inserted into the wider one. Assume the cross-sections of the narrow and wide vessels to be proportional to C_e and C, where C_e and C are the electron and lattice heat capacities, respectively. The electron subsystem is known to have a much smaller heat capacity than the phonon subsystem. Let a fluid flow Q be poured into the narrow vessel; the fluid can flow out from it (through an outlet H_1) into the wide vessel. The cross-section of this outlet is assumed to be proportional to α. The flux of the fluid through a much larger outlet H_2 in the wide vessel simulates heat transfer from the island lattice to the substrate. Then the levels of the fluid in the narrow and wide vessels accumulated at some instant mimic T_e and T, respectively.

Thus, if the fluid is let in at $t = 0$, then in the time interval $\tau_e \sim C_e/\alpha$ a quasi-equilibrium state is established in the narrow vessel at which the whole incoming flux will flow out through the outlet H_1. To attain a high steady-state value of T_e, the flux Q should be sufficiently large

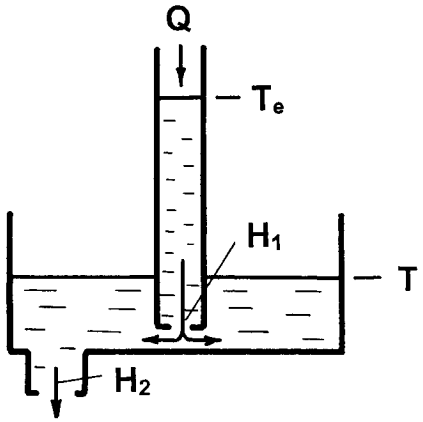

Figure 4. A model of communicating vessels illustrating the electron–lattice energy transfer and nonequilibrium heating of the electron gas in a small particle on a substrate. See text for explanations.

(depending on α). On the other hand, the magnitude of T should not exceed the destruction limit determined by melting and/or evaporation of the particle.

In bulk metals, owing to high electron concentration, the α value is much higher and, hence, Q should also be much larger. Electrons are rapidly heated in a time interval of about $\tau_e \sim C_e/\alpha \sim 10^{-12}$ s, but within a time of $\tau_{ph} \sim C/\alpha \sim 10^{-10}$ s the phonon temperature becomes equal to T_e, and the metal will be melted and evaporated. This is the reason why experimental observations of hot electrons in bulk metals have been reported only for time intervals $\tau_e < t < \tau_{ph}$, e.g. when samples are irradiated by short and intense laser pulses [27].

In IMFs, there are three important distinctions from this situation [19–24]: (i) for a metal particle whose dimensions are smaller than the electron mean free path, the coefficient α is reduced by orders of magnitude in comparison with the bulk metal; (ii) considerable power densities can be pumped into small metal particles; (iii) an island having a good heat contact with the dielectric substrate is able to pass intense energy fluxes without being destructed, and its thermal stability increases as the size is reduced.

Let us discuss these features in more detail. It is known that the major channel of energy losses of electrons in condensed media occurs via generation of acoustic waves by the Cherenkov mechanism [28]. An electron whose velocity v is much higher than the sound velocity s generates an acoustic wave which can be described by the equation

$$\frac{\partial \bar{U}}{\partial t^2} - s^2 \Delta \bar{U} = -\frac{W}{\rho} \Delta \delta(\bar{r} - \bar{v}t) \equiv \bar{F}(t) \tag{2}$$

where U is the longitudinal component of the displacement vector, ρ is the density and W is an interaction coefficient. Equation (2) can be easily solved in the Fourier representation:

$$\bar{U}(\omega, \bar{k}) = \frac{1}{(2\pi)^3} \frac{W}{\rho} \frac{\mathrm{i}\bar{k}\delta(\omega - \bar{k}\bar{v})}{\omega^2 - k^2 s^2}. \tag{3}$$

It is seen that a resonant excitation of acoustic waves is possible at the frequency $\omega = ks$ (the Cherenkov mechanism). However, this excitation cannot occur if the driving force $F(t)$ in equation (2) has a zero Fourier component at the resonance frequency. Just such a situation exists in a metal particle when its size L is smaller than the electron mean free path. Then

the electron trajectory, instead of being a straight line $r(t) = vt$, becomes oscillating with the frequency $f = v/L$, which is due to successive reflections of the electron from the particle surface. In this case the force $F(t)$ should have harmonics only at frequencies which are multiples of f. The resonant excitation of acoustic vibration will be impossible if the frequency $f_F = v_F/L$ (v_F is the Fermi velocity $\sim 10^8$ cm s^{-1}) is higher than the Debye frequency $f_D \sim 10^{13}$ s^{-1}, i.e. the highest frequency of the lattice vibrations. It is readily seen that the condition $f_F > f_D$ is fulfilled for small islands ($L < 10^{-6}$ cm). In such islands, the major mechanism of energy losses operating in bulk samples and large islands vanishes, and the surface scattering of electrons becomes dominating. A theory of surface energy losses [20] predicts the corresponding α value to be by a factor of $\sim 10^2$ lower than its volume value inherent to bulk metals. This estimation has been supported experimentally [29].

Consider now the factors which permit pumping high power densities into small metal particles in IMFs, i.e. providing high Q values in equation (1). In the case of conduction current pumping, the release of a high specific power in some islands results from the very high current density in the conductive channels. The high Q values under CO_2 laser irradiation ($\lambda = 10.6$ μm) are due to enhanced IR optical absorption by small metal particles, which depends very critically on their shape [23]. As follows from equation (1), small values of α and high values of Q give rise to a high electron temperature T_e.

The high thermal stability of small islands is caused by the circumstance that the heat from the island crystal lattice is effectively drained off to the substrate lattice. This differs radically from the situation in bulk metals where the phonon system accepting the thermal load has the same volume as the electron system.

The lattice temperature of an island is [19]

$$T \approx Q V_0 \frac{L}{S_c K} \tag{4}$$

where V_0 is the island volume, S_c the area of the thermal contact with the substrate and K the coefficient of the substrate heat conductivity. As follows from (4), the phonon temperature strongly depends on island dimensions: T is proportional to L^2, since $V_0 \propto L^3$ and $S_c \propto L^2$. For this reason, a small island, without being melted, can transmit, i.e. absorb by the electron subsystem and transfer to the island + substrate phonon bath, a much higher power than the same volume in the bulk metal.

The physical reasons listed above permit the electron gas in small metal particles to be heated in a quasi-steady state to thousands of kelvin while the crystal lattice remains essentially cold. This brings about a variety of specific effects in IMFs.

4. Experimental results and discussion

4.1. Electron and light emission from island films excited by the conduction current

A typical dependence of the emission current on the voltage applied to the film is shown in figure 1. As mentioned in section 2, two alternative mechanisms of the emission have been proposed: the field emission and emission of hot electrons. The former model assumes that rather high electric fields exist in the narrow gaps between the islands [17, 30]. To support this interpretation, it is argued that in a number of experiments the dependence of the emission current, I_e, on the voltage applied to the film, U, appears linear when plotted in the Fowler–Nordheim ('field-emission') coordinates $\log(I_e/U^2)$ versus $1/U$ (it is tacitly assumed that a constant part of the conduction current is extracted to the anode). However, the field emission model was found to be in poor agreement with experimental data on the

temperature dependence of the electron emission as well as on the effect of overlayers and of the deformation of the substrate supporting the island film (see [2, 30, 31] for details).

The model of hot electrons also considers the tunnelling of electrons between the islands. However, in contrast to the field emission model, a sufficiently high transparency of the potential barriers is ascribed just to small interisland spacings rather than to the effect of the external electric field. A theoretical treatment of the electron heating has shown that the emission current should be a linear function in the coordinates $\log I_e$ versus $1/P^{1/2}$, where P is the power pumped into the island [18, 25]. This prediction is corroborated by experimental results [14].

An additional possibility to test both the models is given by experimental data on the electron energy distributions, the electron emission stimulated by infra-red irradiation and the light emission from IMFs. From the electron energy distributions, the electron gas temperature within the emission centers was estimated at a few thousand kelvin [9, 32]. This value agrees with the theoretical predictions of the model of hot electrons and with the electron temperatures evaluated by other methods [9, 32–35]. In particular, the evaporation of BaO overlayers onto island films was found to lead to a significant increase of the conduction current and to a much stronger (by several orders of magnitude) growth of the emission current [5]. Both the effects can be ascribed to the reduction of the work function of the islands. Assuming that the electron emission from IMFs is the Richardson emission of the hot electrons, the work function dependence of the emission current was used to estimate T_e and a value of $T_e \approx 2 \times 10^3$ K was obtained.

4.2. IR-laser-induced electron emission from island films

Electrons and photons are emitted from IMFs when a sufficient power is pumped into the islands, not only by passing a current through the film, but also by various other means of excitation, in particular by laser irradiation.

For infra-red laser excitation, the films were evaporated onto oxidized Si substrates which are transparent to the CO_2 laser radiation. A pulsed CO_2 TEA-laser ($\lambda = 10.6$ μm, $\tau = 0.2$ to 1.0 μs, $f_r = 1$ to 30 Hz) was used. The laser beam was incident onto the rear of the island film emitter through a Si window in an evacuated device. Then it passed through the substrate and interacted with the island film (figure 5(a)). A measurable emission current from a gold island film appears at a power density of the laser beam of $\sim 10^4$ W cm^{-2} [36] whereas for bulk Au this value must be above $\sim 10^7$ W cm^{-2} [37]. No significant change in the shape of Au islands is apparent below 2×10^5 W cm^{-2}. Above this value, one first observes the evaporation of comparatively large Au islands ($\sim 10^2$ nm) while smaller islands stand up to much higher powers. The stability of IMFs increases when they are prepared from refractory materials [14].

The time lag between the laser and electron emission pulses is below 2×10^{-8} s at low and medium power densities. This lends support to the model ascribing the electron emission to the fast generation of hot electrons in nanoparticles (section 3). However, the lag becomes appreciable at high power densities when the film is gradually destroyed because of evaporation of the metal islands. Probably, the classical (equilibrium) thermionic emission comes into effect in this case. At low and medium laser power densities P, the emission current I_e as a function of the power density of the laser beam is linear in coordinates $\log I_e$ versus $1/\sqrt{P}$ (figure 5). This also agrees with the model of hot electrons. On the other hand, the photoelectric effect (both one-photon and many-photon) can be excluded in this case since the work function of the metals studied (4.5 to 5.0 eV) is about 40 times as high as the energy of quanta in the CO_2 laser beam ($h\nu = 0.12$ eV).

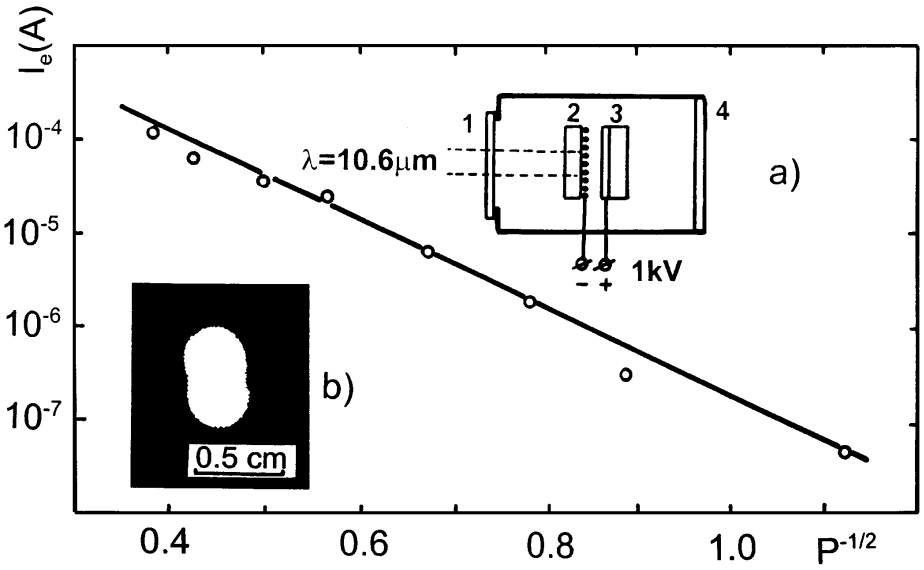

Figure 5. Straight line: logarithm of the electron emission current from a gold island film on Si excited by a CO_2 laser as a function of $P^{-1/2}$. The laser beam power density P is measured in units 10^5 W cm^{-2}. Insets: (a) schematic of an IR electron-optical image converter using an IMF cathode (1 is an Si entrance window, 2 the cathode, 3 a cathodoluminescent screen and 4 a glass window); (b) a visualized profile of an IR laser beam.

4.3. Light emission from island metal films

The light emission from IMFs sets in simultaneously with the electron emission [1, 9]. Here we will consider the light emission from IMFs which occurs under conduction current excitation. We recall that both electrons and light are emitted from the same centres [38]. The existence of several intensity maxima in the light emission spectra (figure 6) may suggest that a few radiation mechanisms operate in parallel. Theoretically, one can predict that the light emitted by IMFs contains contributions from intraband quantum transitions, bremsstrahlung, inverse surface photoeffect and plasmon-mediated radiation (the plasmons being generated both in inelastic tunnelling and by hot electrons).

The above data can be compared with light emission spectra measured for other related systems. In particular, there is an obvious similarity between a pair of adjacent metal islands on a dielectric substrate, a metal–insulator–metal (MIM) structure and a tunnel gap in STM. The light emission from MIM tunnel junctions has been investigated in many works (see e.g. [39] and references therein). The spectra obtained have been attributed mainly to the radiative decay of surface plasmon–polariton modes excited by inelastic electron tunnelling. There are also experimental arguments in favour of the radiative decay of surface plasmons that are generated by hot electrons injected into one of the metal electrodes without energy loss in the tunnelling gap [40].

A light emission spectrum of an Ag IMF having a single light emitting centre is juxtaposed in figure 6 with a spectrum of an Ag–Ag(111) tunnel gap in STM [41]. A rather close similarity in some features of the spectra is evident. The photon emission spectra recorded in STM are interpreted in terms of radiative decay of tip-induced plasmon modes excited in inelastic

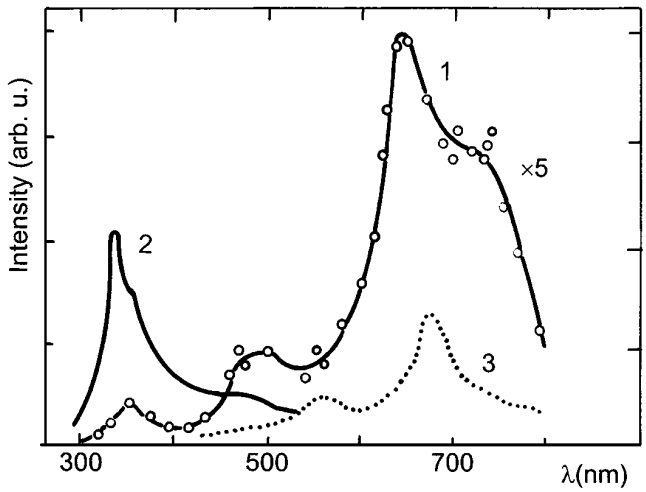

Figure 6. Light emission spectra: (1) for an individual emitting centre in a silver IMF excited by conduction current; (2) for the same film excited by electron bombardment (50–200 eV); (3) for an Ag-tip/Ag(111) tunnel gap [41].

electron tunnelling (see e.g. [42]). Similar localized plasmons can form and decay in the tunnel gap between the adjacent nanoislands. The radiation spectrum of the IMF has also an ultraviolet peak ($\lambda \approx 350$ nm, $h\nu = 3.5$ eV) which coincides with the maximum in the photon radiation observed under electron bombardment of the Ag island film from an external electron source. Thus several maxima seen in the spectra of IMFs may indicate the operation of diverse physical mechanisms of light emission. This possibility can originate from the hot electrons which are able to induce electromagnetic radiation due to various effects.

When an IMF is covered with a BaO submonolayer, the intensity of the emitted light increases while its spectrum remains almost unchanged [5]. On the other hand, stearone and some other organic overlayers bring about more substantial changes in IMFs characteristics. In particular, they can cause the occurrence of N-shaped conduction current–voltage curves ('voltage-controlled negative resistance', or VCNR) (figure 7) [5]. There are observations suggesting that organic molecules evaporated onto IMFs *in the presence of applied voltage* can polarize and self-assemble into thin quasi-polymeric bridges which span the gaps between the islands. As a consequence, the VCNR region in the conduction current–voltage characteristics can arise through one of the mechanisms suggested for switching phenomena in semiconductors: thermal (structural), electronic or combined ones [43]. Figure 7 displays also the light emission intensity recorded in the alternating voltage regime. It is seen that the hysteresis loop for the light intensity mirrors rather closely the modulus of the derivative of the conduction current loop. Such a behaviour is quite typical for electroluminescence of semiconductors [44]. We suppose that the electroluminescence of organic bridges may be excited by hot electrons injected into them from adjacent metal islands.

The results presented in this section demonstrate the close correlation between the intensities of the electron and light emission from IMFs and thus evidence that a unified explanation should exist for both phenomena.

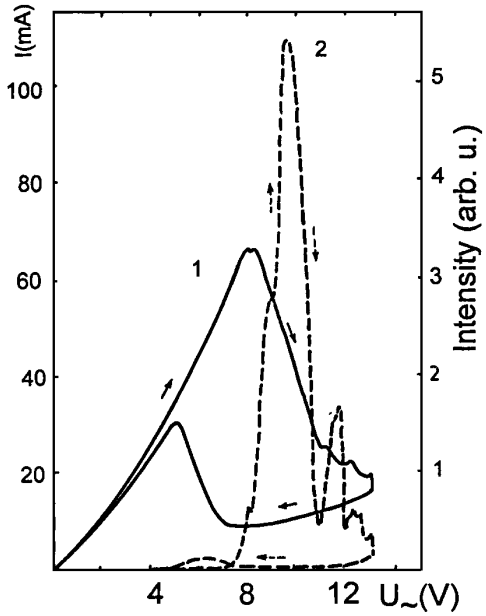

Figure 7. Hysteresis loops for the conduction current (1) and light intensity at $\lambda = 615$ nm (2) recorded for an Au film covered with stearone. Voltage frequency: 500 Hz. Sweep time: 2 min [5].

5. Examples of applications of island metal films

The phenomenon of electron emission from IMFs induced by passing current through them has been utilized to develop 'cold' cathodes for vacuum microelectronic devices. Such devices are known to combine the advantages of vacuum electronics and solid-state electronics (fast operation + smallness + high radiation stability $+\cdots$). A technology has been elaborated allowing the fabrication of gold IMF cathodes (activated by BaO) with an emission current $\sim$10 μA stable for about 5000 hours in the continuous operation mode [45]. Still higher parameters have been achieved with IMF cathodes based on Mo and other refractory metals [46].

Large-area IMF emitters can be fabricated either by evaporation of the film between two comb-shaped contact electrodes inserted into each other [47] or by making a matrix cathode. In particular, recent publications of Japanese workers have presented a 10 in full colour flat cathodoluminescent display ($\approx$10 mm thick) using a matrix cathode which they name 'the surface conduction emitter' [3]. The emitter was fabricated of fine PdO particles using an ink-jet printing process carried out in air. Its micrographs show that the size of the particles is about 5–10 nm, so it actually is an island film emitter. Such displays are expected to substitute traditional bulky cathode-ray tubes in many applications.

Island thin films have also been utilized for visualization of the spatial power distribution of infrared laser radiation [48] (figure 5). The spatial power distribution in the laser beam is mirrored in the distribution of the electron emission current density over the IMF cathode and is displayed on the cathodoluminescent screen.

There have also been reports about the development of IMF based tensometers (see e.g. [30, 49], and microsources of light [50].

6. Conclusions

The available data on electron and photon emission from IMFs seem to agree well with the model which predicts a strong nonequilibrium heating of the electron gas in nanoparticles. Their size is so small that the scattering of electrons occurs mainly at the particle surface. The result is a strong suppression of the electron–lattice energy transfer, which provides a favourable possibility for stationary generation of hot electrons when a sufficient power is pumped into the particle. Thus the metal island films differ sharply from bulk metals where hot electrons can be generated only for very short times.

The application potentialities of IMFs range from microcathodes and microsources of light to large-area matrix cathodes for flat information displays. It is also appropriate to note that hot electrons can effectively stimulate surface chemical reactions [51–53]. Hot electrons are also known to play an important part in semiconductor nanostructures [54]. Thus a deeper insight into the mechanisms of generation of hot electrons in nanoparticles is important to better understand the properties of diverse dispersed systems fed with energy.

It should be expected that recent and future advances in nanotechnologies will open new possibilities in the preparation and investigation of the island films with more controllable parameters.

Acknowledgments

This work was supported in part by the Ministry of Ukraine for Science and Technologies (grant No 2.4/790). AGN also gratefully acknowledges the support in the framework of the International Soros Science Education Program through grant No SPU072041. We are indebted to Mrs O L Fedorovich and Mr O E Kiyayev for their help in the preparation of the typescript.

References

[1] Borziak P G, Sarbej O G and Fedorovich R D 1965 *Phys. Status Solidi* **8** 55
[2] Borziak P G and Kulyupin Yu A 1980 *Elektronnye Processy v Ostrovkovykh Metallicheskikh Plenkakh [Electron Processes in Island Metal Films]* (Kiev: Naukova Dumka) (in Russian)
[3] Yamaguchi E *et al* 1997 *J. Soc. Inform. Display* **5** 345
[4] Tognini P, Andreani L C, Geddo M, Stella A, Cheyssac P, Kofman R and Miglori A 1996 *Phys. Rev.* B **53** 6992
[5] Borziak P G, Dan'ko D B, Fedorovich R D, Kiyayev O E and Naumovets A G 1996 *Prog. Surf. Sci.* **53** 171
[6] Alekseenko B V and Fedorovich R D 1982 *Thin Solid Films* **92** 252
[7] Alekseenko B V, Tomchuk P M and Fedorovich R D 1988 *Poverkhnost Fiz. Khim. Mekh.* **10** 42
[8] Neugebauer C A and Webb M B 1962 *J. Appl. Phys.* **33** 74
[9] Borziak P G, Kulyupin Yu A, Sarbei O G and Fedorovich R D 1969 *Ukr. Fiz. Zh.* **14** 395
[10] Alekseenko B V, Tomchuk P M and Fedorovich R D 1987 *Mater. Sci.* **13** 161
[11] Bardamid A F, Kulyupin Yu A, Pilipchak K N and Shaldervan A I 1972 *Dispersed Metal Films* (Kiev: Institute of Physics) (in Russian)
[12] Nepijko S A and Styopkin V I 1983 *Poverkhnost Fiz. Khim. Mekh.* **1** 54
[13] Fedorovich R D, Naumovets A G, Ostranitsa A P and Tomchuk P M 1990 *Int. J. Electron.* **69** 179
[14] Viduta L V, Kiyayev O E, Naumovets A G, Ostranitsa A P and Fedorovich R D 1991 *Radiotekh. Elektron.* **36** 1345
[15] Rosenfeld G, Morgenstern K, Beckman I, Wulfhekel W, Laegsgaard E, Besenbacher F and Comsa G 1998 *Surf. Sci.* **402–404** 401
[16] Chen W and Ahmed H 1998 *Adv. Imaging Electron Phys.* **102** 87
[17] Dittmer G 1972 *Thin Solid Films* **9** 317
[18] Tomchuk P M and Fedorovich R D 1966 *Sov. Phys.–Solid State* **8** 226
[19] Belotskii E D and Tomchuk P M 1990 *Surf. Sci.* **239** 143
[20] Belotskii E D, Luk'yanets S P and Tomchuk P M 1992 *Sov. Phys.–JETP* **74** 88
[21] Fedorovich R D, Naumovets A G and Tomchuk P M 1993 *Prog. Surf. Sci.* **42** 189

[22] Fedorovich R D, Kiyayev O E, Nauvomets A G, Pilipchak K N and Tomchuk P M 1994 *Phys. Low-Dim. Struct.* **1** 83
[23] Tomchuk P M and Tomchuk B P 1997 *Sov. Phys.–JETP* **85** 360
[24] Fedorovich R D, Naumovets A G and Tomchuk P M *Phys. Rep.* at press
[25] Tomchuk P M and Fedorovich R D 1966 *Sov. Phys.–Solid State* **8** 2510
[26] Tomchuk P M 1979 *Ukr. Fiz. Zh.* **24** 182
[27] Anisimov S I, Benderskii V A and Farkash D 1977 *Usp. Fiz. Nauk* **122** 185
[28] Buckingham M J 1953 *Proc. Phys. Soc.* **66** 601
[29] Gorban S A, Nepijko S A and Tomchuk P M 1991 *Int. J. Electron.* **70** 485
[30] Kulyupin Yu A and Nepijko S A 1975 *Fiz. Tverd. Tela* **17** 2747
[31] Araki H and Hanawa T 1988 *Thin Solid Films* **158** 207
[32] Kulyupin Yu A, Nepijko S A and Styopkin V I 1982 *Izv. Akad. Nauk USSR, Ser. Fiz.* **46** 2354
[33] Borziak P G, Kulyupin Yu A and Nepijko S A 1976 *Thin Solid Films* **36** 235
[34] Viduta L V and Kulyupin Yu A 1979 *Radiotekh. Electron.* **24** 823
[35] Bischoff M, Pagnia H and Trickl J 1992 *Int. J. Electron.* **73** 1009
[36] Benditskii A A, Viduta L V, Kulyupin Yu A, Ostranitsa A P, Tomchuk P M, Fedorovich R D and Yakovlev V A 1986 *Izv. Akad. Nauk SSSR Ser. Fiz.* **50** 1634
[37] Anisimov S I, Kopeliovich B L and Perelman G L 1974 *Zh. Eksp. Teor. Fiz.* **66** 776
[38] Kulyupin Yu A and Pilipchak K N 1972 *Phys. Status Solidi* a **11** K15
[39] Dawson P, Walmsley D G, Quinn H and Ferguson A J L 1984 *Phys. Rev.* B **30** 3164
[40] Kirtley J R, Theis T N, Tang J C and Di Maria D J 1983 *Phys. Rev.* B **27** 4601
[41] Berndt R, Baratoff A and Gimzewski J K 1990 *Scanning Tunneling Microscopy and Related Methods (NATO ASI Series E 184)* ed R J Behm, N Garcia and H Rohrer (Dordrecht: Kluwer) p 269
[42] Berndt R and Gimzewski J K 1992 *Surf. Sci.* **269/270** 556
[43] Owen A E, Le Comber P G, Hajto J, Rose M J and Snell A 1992 *J. Int. J. Electron.* **73** 897
[44] Ono Y A 1995 *Electroluminescent Displays* (Singapore: World Scientific)
[45] Sukharier A S 1974 *Nenakalivayemye Katody (Nonheated Cathodes)* ed M I Elinson (Moscow: Sovietskoye Radio) p 39 (in Russian)
[46] Borziak P G, Viduta L V, Kandyba P E, Kolesnikov D P, Kostenko A D, Kulyupin Yu A, Fedorovich R D and Yastrebov V G 1973 *Izv. Akad. Nauk SSSR Ser. Fiz.* **37** 2613
[47] Fedorovich R D, Naumovets A G and Tomchuk P M 1996 *Condens. Matter Phys.* **7** 5
[48] Benditskii A A, Danko D B, Fedorovich R D, Nepijko S A and Viduta L V 1994 *Int. J. Electron.* **77** 985
[49] Nepijko S, Schulze W, Rabin I and Viduta L 1998 *Ann. Phys., Lpz.* **7** 101
[50] Kulyupin Yu A, Pilipchak K N and Fedorovich R D 1986 *Bull. Inventions USSR* No 40, certificate No 1279433
[51] Gadzuk J W, Richter L J, Buntin S A, King D S and Cavanagh R R 1990 *Surf. Sci.* **235** 317
[52] Sharpe R G, Dixon-Warren St J, Durston P J and Palmer R E 1995 *Chem. Phys. Lett.* **234** 354
[53] Gadzuk J W 1997 *J. Vac. Sci. Technol.* A **15** 1520
[54] Shah Jagdeep (ed) 1992 *Hot Carriers in Semiconductor Nanostructures: Physics and Applications* (San Diego: Academic)